

Evaluation of Radiological Risk Parameters in the Soil along the Coastline of Arin Lake (Bitlis)

Şule KARATEPE ÇELİK^{1*}, Sultan ŞAHİN BAL²

¹Bitlis Eren University, Vocational School of Hizan, Bitlis, Turkey

²Bitlis Eren University, Department of Physics, Bitlis, Turkey

Received on 23 June 2025; Accepted on 25 December 2025

Abstract

This study examines natural (²³⁸U, ²³²Th, and ⁴⁰K) and artificial (¹³⁷Cs) radioactivity concentrations in 27 soil samples collected from the Arin Lake (Bitlis) coastline using an HPGe detector. For this purpose, dose calculations were performed, based on the radioactivity concentrations in the soil samples. The mean radioactivity concentration of ²²⁶Ra, ²³²Th, ⁴⁰K, and ¹³⁷Cs were 34.73±0.75, 32.43±0.67, 529.28±11.78, and 8.46±0.17 Bq.kg⁻¹, respectively. The radiological parameters with Ra equivalent (Rae_q) value, the annual effective dose, and the absorbed dose values were lower than the recommended world mean. Furthermore, the radiological hazard indices Hin, Hex, and ELCR were below the specified limit values. In addition, the findings were compared to similar research in several other countries.

© 2026 Jordan Journal of Earth and Environmental Sciences. All rights reserved

Keywords: Radioisotopes, dose rates, Arin Lake, hazard indices

1. Introduction

The living are continuously exposed to radiation from natural radioactive sources throughout their lives. This exposure arises from naturally occurring radioactive materials (NORMs) found in various components of Earth's environment, such as soil, water, and the atmosphere. Humans, as well as other living organisms, come into contact with these sources in their daily activities, leading to an inevitable accumulation of background radiation throughout their lifetimes (UNSCEAR 2000; Kuluöztürk et al., 2020; Özveren et al., 2020; Al-Momani et al., 2024). Naturally occurring radioactive materials (NORMs) such as ²²⁶Ra, ²³²Th, and ⁴⁰K are the radioisotopes that contribute most to background radiation. These radionuclides are produced by the natural decay of elements like uranium, thorium, and potassium in the Earth's crust (Baykara et al., 2011; Ibraheem et al., 2018; Abbasi et al., 2023; Yadav et al., 2023). Radioactivity levels differ from one location to another, owing to distinct geographical conditions and geological structures. For example, regions that contain uranium- or thorium-rich minerals tend to have higher levels of background radiation. In comparison, areas with different geological characteristics may show lower levels of natural radioactivity. (Özden et al., 2021; Yadav et al., 2023). Furthermore, artificial radioactive substances arise from nuclear weapon trials, accidents in nuclear reactors, and other nuclear studies. Among these, ¹³⁷Cs is of particular importance due to its long half-life and its impact on internal irradiation. These artificial sources have raised concerns about their long-term impacts on both ecosystems and human health (Kobyas et al., 2015).

Regarding this subject in recent years, there has been extensive research into assessing the levels of radioactivity

in soil, water, sand, and various food sources (UNSCEAR 2000; Ibraheem et al., 2018; Mehra et al., 2021; Tucakovic et al., 2023; Akça et al., 2014; Cambazoğlu et al., 2018). These studies are crucial for determining baseline radioactivity levels, which help in identifying regions with unusual radiation levels caused by natural variations or human activities (Tucakovic et al., 2023; Al-Harabsheh et al., 2020). Especially, many studies have been conducted to evaluate the natural and artificial radioactivity levels in soil samples collected from rivers, lakes, and coasts from different regions of the world (Kuluöztürk et al., 2020; Shadrin et al., 2020; Singh et al., 2021; Mantero et al., 2020; Al Shaaibi et al., 2023).

Lakes are vital water sources for aquatic life and humans. Lakes reflect the geological structure of the region in which they are located (Singh et al., 2021). The composition of soil along the lake coast is shaped by the lake's formation process and various atmospheric phenomena. The primary factor contributing to the radioactivity levels observed in sediment and coastal soil compositions in lakes is the presence of radioisotopes, such as ²³⁸U, ²³²Th, and ⁴⁰K in the soil and rocks. (Kobyas et al., 2015). These radionuclides naturally occur in the Earth's crust, and their levels in lake ecosystems are influenced by surrounding geology and external environmental conditions (Baykara et al., 2011). These radioisotopes found in the soil contribute to the radioactive background level within the lake ecosystem. Though background radiation is low in intensity, continuous exposure can have lasting ecological impacts, particularly in environments where organisms are regularly exposed.

The objective of the study is to investigate both natural and artificial radioactivity levels in soil along the shoreline of Lake Arin. The study also aims to compare radioactivity

* Corresponding author e-mail: skaratepe@beu.edu.tr

concentrations in lakes, rivers, and coastal areas across different regions of the world and to identify areas that may pose radiological hazard indices. This research is driven by the need to track and comprehend the long-term effects of radiation exposure on ecosystems and human populations.

2. Materials and Methods

2.1. Study area

Arin Lake, located in the east of Türkiye, is within the borders of Bitlis province (Figure 1). It is located at 42°98' E and 38°45' N. This soda lake is situated south of the volcanic

Nemrut Mountain and is surrounded by three villages. The lake serves as a breeding habitat for the endangered White-headed Duck, and it is recognized as a migratory route for numerous bird species. During the migration season, the most notable avian visitors include songbirds and flamingos (Nergiz & Durmuş, 2017). Furthermore, during the Ottoman period, soda production was carried out using resources from both Lake Van and Lake Arin, owing to the soda-rich nature of Lake Arin (Çelik & Bal, 2024).

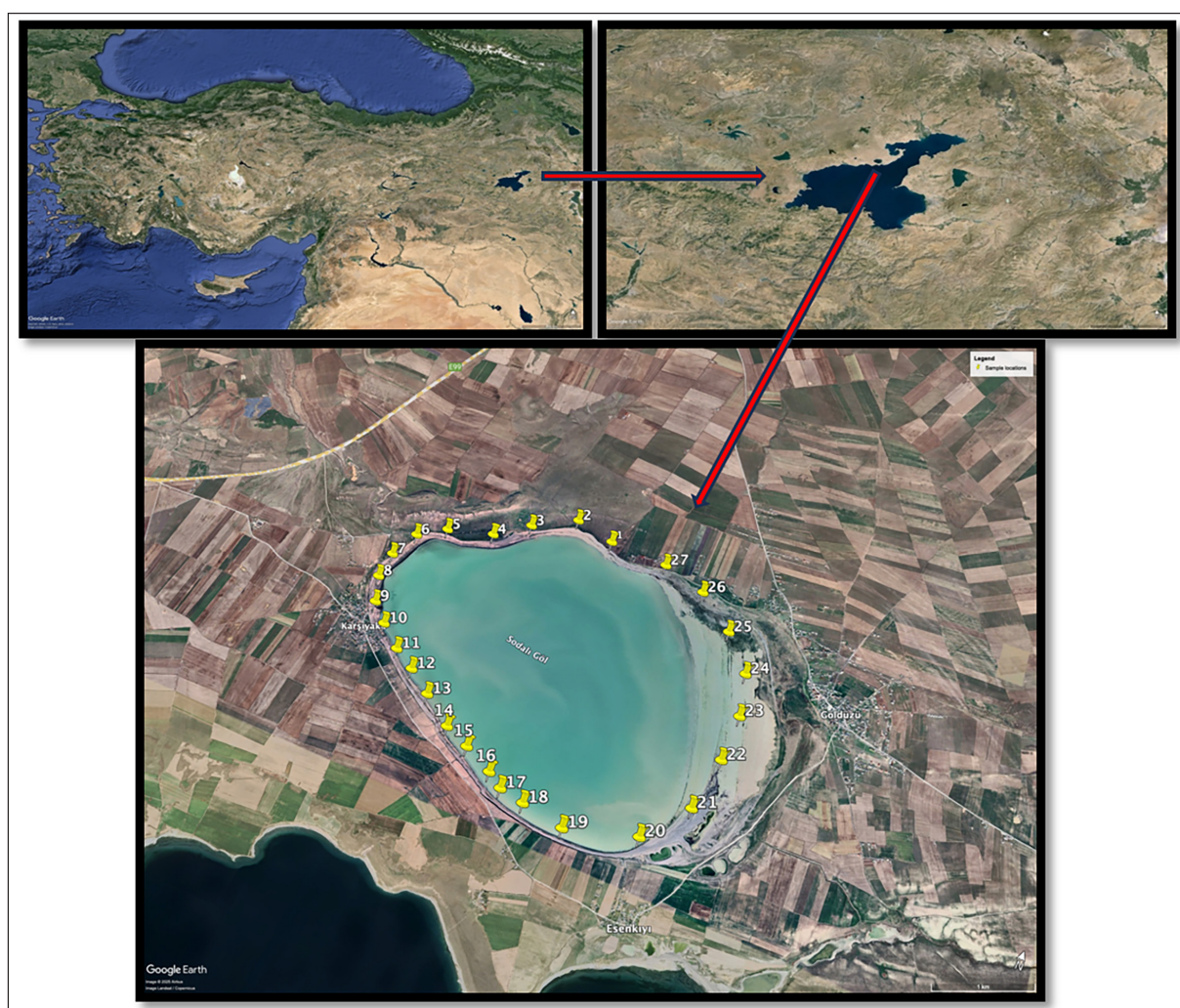


Figure 1. Map of the study area and location of the soil sample points.

2.2. Sampling and sample preparation

Twenty-seven soil samples were collected from Arin Lake and its surrounding areas. Figure 1 shows the sample locations from which they were obtained. The sample locations were determined using GPS. For soil samples, samples were collected from a depth of 10 to 15 cm below the surface (Satyanarayana et al., 2023). Additionally, each soil sample was dried before assessing activity levels. Roughly 1 kg of each sample was transferred to the laboratory and labeled for identification. To prevent any alteration in the physical and chemical characteristics of the samples, all the samples were dried at 80°C for 24 h to remove moisture (IEAE 2003; Van et al., 2019). The samples were sieved through a 60-mesh screen for homogenous (Kuluöztürk et

al., 2020). When using a germanium detector, it is important that the particle size is equal and the sample is homogeneous. All samples were placed in 1 kg Marinelli containers suitable for measurement with a germanium detector.

2.3. Gamma Spectrometric Analysis

Radioactivity measurements of soil samples were performed using a high-purity gamma-ray detector system with a coaxial p-type HPGe detector (GEM50P4-83). It can measure gamma rays with energies between 40 keV and 10 MeV (Karakaya et al., 2015). Relative efficiency is at least 50%, and the separation power is 1.90 keV at 1.33 MeV for ^{60}Co (FWHM). The detector is enclosed within a 10 cm-thick cylindrical lead shield to reduce background radiation (Karakaya et al., 2015). Additionally, lead shielding includes

a 1.5 mm thick copper and a 1 mm thick tin layer to stop the X-rays. Analysis was performed with MAESTRO32 (ORTEC) software (ORTEC 2006). Energy and efficiency calibrations were completed using standard sources (IAEA-375) obtained from the IAEA (Gilmore, 2008). Energy and efficiency calibrations of the detector were performed using a standard multi-nuclide gel source with a known activity of 1.365 μCi , containing isotopes such as ^{57}Co , ^{60}Co , ^{88}Y , ^{109}Cd , ^{139}Ce , ^{137}Cs , ^{203}Hg , ^{210}Pb , and ^{241}Am . The measurements were taken at 43,200-second (24-hour) intervals. The efficiency vs. energy graph is plotted and adjusted to fit the following equation (Kayakökü & Dogru, 2017; Özmen et al., 2014).

$$E_{ff}(E) = a + b \times \log \log (E)^2 + d \times \log \log (E)^3 \quad (1)$$

where a, b, c, and d are the optimal parameters identified by the fitting algorithm. Finally, the efficiency values required for calculating the activity concentration of the full-energy peaks were derived using this equation.

Each sample was counted for 50000 s to get acceptable counting data. ^{226}Ra , ^{232}Th , and ^{40}K isotopes were determined through the examination of gamma-ray lines at specific energy levels: 351.9 keV (^{214}Pb) and 609.3 keV (^{214}Bi) for ^{226}Ra , 911.2 keV (^{228}Ac) for ^{232}Th , 1460.8 keV for ^{40}K . Observation was made at 661.7 keV to detect the ^{137}Cs isotope, which is an artificial radionuclide.

2.4. Radioactivity Concentration and Dose Calculations

The activity levels in samples were determined with the subsequent formula:

$$A(\text{Bq.kg}^{-1}) = \frac{N_S - N_B}{\varepsilon \times P_\gamma \times t} \times \frac{1}{m} \quad (2)$$

Where are counted per second (cps) for the sample and background, respectively. ε is the detector efficiency, P_γ is the γ -abundance, t is the counting time (50000 s), and m is the sample mass of 1kg (Kuluöztürk et al., 2020; Cambazoğlu et al., 2018).

The calculation of minimum detectable activities (MDA) was performed utilizing the following equation:

$$MDA(\text{Bq.kg}^{-1}) = \frac{2.71 + 4.65\sqrt{N_B}}{\varepsilon \times P_\gamma \times t} \quad (3)$$

Where N_B is represented by the net peak areas in a specific energy range for the background, ε is the detector efficiency, and A is the abundance associated with the energy, and t is counting time.

The calculated Ra equivalent value, which includes the weighted contributions from Ra, Th, and K, is an important parameter for comparing activity concentrations across all data. It was computed employing the following equation.

$$Ra_{eq}(\text{Bq.kg}^{-1}) = A_{Ra} + 1.43A_{Th} + 0.077A_K \quad (4)$$

Where, A_{Ra} , A_{Th} , and A_K represent the respective activity values for ^{226}Ra , ^{232}Th , and ^{40}K . The maximum recommended value of Ra_{eq} is 370 (UNSCEAR 2000).

To assess the attributes of gamma radiation in outdoor environments, the absorbed dose rate (D) in outdoor air, measured 1 meter above the ground, was computed from the activities of ^{238}U , ^{232}Th , and ^{40}K using the following formula:

$$D(\text{nGy/h}) = 0.462C_U + 0.604C_{Th} + 0.417C_K \quad (5)$$

Where C_K , C_{Th} , and C_U represent the concentrations of ^{40}K , ^{232}Th , and ^{238}U activities, respectively.

Annual effective dose rate (AED) was defined as the value of radiation exposure to an individual over a year and provides an assessment of the potential health hazards associated with this radiation exposure (UNSCEAR 2000; Baykara et al., 2011)

$$AED(\text{mSv/y}) = D(\text{nGy/h}) \times 8760(\text{h/y}) \times 0.2 \times 0.7(,) \quad (6)$$

Where 0.2 is the outdoor time conversion factor, and 0.7 stands for the dose conversion factor in Sv to Gy. The global mean annual effective dose (AEDE) of outdoor terrestrial gamma radiation is 70 $\mu\text{Sv.y}^{-1}$ (UNSCEAR 2000; Al Shaaibi et al., 2023).

The external and internal hazard index (Hex) was calculated from the formula as follows (Krieger, R., 1985, Abbasi, 2023):

$$H_{ex} = \frac{A_{Ra}}{370} + \frac{A_{Th}}{259} + \frac{A_K}{4180} \leq 1 \quad (7)$$

$$H_{in} = \frac{A_{Ra}}{185} + \frac{A_{Th}}{259} + \frac{A_K}{4180} \leq 1 \quad (8)$$

Excess lifetime cancer risk (ELCR) was calculated with the following equation:

$$ELCR = AED \times DL \times RF \quad (9)$$

Where AED is the annual effective dose rate ($\mu\text{Sv.y}^{-1}$), DL is the average life (70 years), and, for stochastic effects, RF (0.05 Sv $^{-1}$) is used as the risk factor for cancer per Sievert in the population, as described by ICRP (ICRP 1990).

3. Results and Discussion

The radioactivity concentrations of the natural radioisotopes ^{226}Ra , ^{232}Th , and ^{40}K , and artificial radioisotopes ^{137}Cs in soil samples are given in Table 1 and Figure 2.

The samples exhibited varying levels of activity concentrations, ranging from 9.31 \pm 0.21 to 50.76 \pm 1.05 Bq.kg $^{-1}$ for ^{226}Ra , 48.16 \pm 1.05 to 8.47 \pm 0.18 Bq.kg $^{-1}$ for ^{232}Th , 97.55 \pm 2.46 and 896.13 \pm 17.87 Bq.kg $^{-1}$ for ^{40}K , and 4.41 \pm 0.11 to 18.16 \pm 0.35 Bq.kg $^{-1}$ for ^{137}Cs . The mean values were calculated to be 34.73 \pm 0.75, 32.43 \pm 0.67, 529.28 \pm 11.78, and 8.46 \pm 0.17 Bq.kg $^{-1}$ for ^{226}Ra , ^{232}Th , ^{40}K , and ^{137}Cs , respectively. Examining both Table 3 and Figure 2 concurrently, the average activity concentrations of ^{226}Ra , ^{232}Th , and ^{40}K in the soil samples follow the order $^{226}\text{Ra} < ^{232}\text{Th} < ^{40}\text{K}$. Sample 1 exhibited the highest activity concentrations of ^{226}Ra , ^{232}Th , and ^{40}K , whereas sample 27 exhibited the lowest. The higher radionuclide values observed at sample numbers 1–6 can be attributed to the more pronounced accumulation of fine-grained sediment and chemical retention processes in this area. In soda lake conditions, high alkalinity may facilitate the adsorption of radionuclides into clay and carbonate phases, increasing sediment enrichment. Furthermore, surface runoff and erosion inputs from surrounding settlements and agricultural activities may have contributed to the accumulation of material transported from the basin in this section. The significant difference observed between closely located sampling points suggests micro-scale heterogeneity in the sediment.

Changes in clay and silt fractions can increase the specific surface area and, consequently, the retention of natural radionuclides. Furthermore, mineralogical composition, organic matter, redox conditions, and hydrodynamic deposition and resuspension processes, which depend on the flow regime, can lead to divergent concentrations even over short distances. Therefore, the difference between sample numbers 1 and 27 should not be explained solely by distance but should be evaluated in light of the combined effect of local sedimentological and geochemical conditions. Additionally, the lowest ^{137}Cs activity was obtained from

sample 16. According to the UNSCEAR report, the activity concentrations of ^{226}Ra , ^{232}Th , ^{40}K , and ^{137}Cs have world mean values of 35 Bq.kg^{-1} , 30 Bq.kg^{-1} , 400 Bq.kg^{-1} and 51 Bq.kg^{-1} respectively (UNSCEAR 2000). As seen in Table 1, the ^{232}Th and ^{40}K activity values were slightly higher than these. However, the ^{226}Ra activity concentration was determined to be lower. In addition to natural radioisotopes, ^{137}Cs is an artificial radioisotope. It is emitted following nuclear weapons testing and nuclear power plant accidents. The measured ^{137}Cs activity concentration was lower than the results in the other regions listed in Table 2.

Table 1. Radioisotope activity concentrations of soil samples in Arin Lake

Sample ID	Radioisotopes Activities (Bq.kg^{-1})			
	^{226}Ra (351.9–609.3 keV)	^{232}Th (911,2 keV)	^{40}K (1461,8 keV)	^{137}Cs (662 keV)
1	50.76±1.05	48.16±1.05	896.13±17.87	4.48±0.1
2	41.60±0.83	42.92±0.87	699.83±15.23	6.06±0.13
3	49.35±1.06	44.87±0.94	841.83±15.63	5.93±0.11
4	38.87±0.79	39.53±0.82	704.47±13.52	5.65±0.12
5	44.17±0.92	41.44±0.85	717.43±14.34	8.95±0.19
6	41.92±0.86	42.29±0.89	801.1±17.44	6.42±0.13
7	34±61±0.73	31.51±0.63	531.32±12.69	10.24±0.23
8	26.08±0.55	23.24±0.49	338.62±8.43	7.35±0.15
9	20.83±0.44	19.62±0.42	223.72±5.54	8.82±0.19
10	18.13±0.37	18.48±0.42	191.2±4.87	6.39±0.12
11	29.48±1.10	21.55±0.43	375.31±9.35	6.31±0.12
12	19.09±0.42	18.22±0.39	235.34±5.81	10.63±0.23
13	35.56±0.76	32.22±0.66	512.91±12.83	11.84±0.25
14	28.61±0.59	28.73±0.64	437.36±10.36	5.61±0.11
15	30.90±0.64	29.1±0.56	455.53±10.07	7.37±0.15
16	36.18±0.75	34.33±0.69	512.35±12.3	4.41±0.11
17	32.70±0.67	27.17±0.54	464.9±11.33	7.4±0.14
18	42.83±0.86	41.82±0.85	631.76±12.99	8.12±0.16
19	46.79±0.99	48.11±0.98	710.57±14.46	6.41±0.14
20	40.30±0.83	40.97±0.83	636.26±14.16	10.38±0.21
21	30.95±0.63	28.31±0.59	462.09±11.53	11.86±0.21
22	35.17±0.77	28.57±0.61	521.06±12.22	12.64±0.24
23	32.50±0.68	30.03±0.67	471.19±11.75	18.16±0.35
24	28.36±0.59	25.95±0.56	391.15±9.79	10.9±0.21
25	46.52±0.95	42.39±0.87	731.23±16.25	11.42±0.22
26	46.07±1.31	37.66±0.76	698.43±14.67	7.36±0.17
27	9.31±0.21	8.47±0.18	97.55±2.46	7.19±0.15
Min.	9.31±0.21	8.47±0.18	97.55±2.46	4.41±0.11
Max.	50.76±1.05	48.16±1.05	896.13±17.87	18.16±0.35
Mean	34.73±0.75	32.43±0.67	529.28±11.78	8.46±0.17
¹ World mean	35	30	400	51

¹(UNSCEAR 2000)

Additionally, it has been determined that similar results were obtained when comparing the activity concentrations of ^{40}K , ^{226}Ra , and ^{232}Th in this research with those in several other countries, as presented in Table 2. Table 2 reveals wide variability in naturally occurring radionuclides reported in lake and coastal sediments across different geographical regions. In particular, the findings for ^{226}Ra and ^{232}Th are generally at a similar level to values reported in different aquatic environments such as Lake Eğirdir and the East

Siberian Sea. They are consistent with the ranges reported for Lake Erçel and the Aegean coast. In contrast, ^{40}K is higher than the lower levels reported in Brazil; this may be related to the sediment's mineralogical composition and potassium-rich lithological inputs.

The frequency distribution of radionuclides ^{226}Ra , ^{232}Th , ^{40}K , and ^{137}Cs is illustrated in Figure 2. The histogram graphs in Figure 2 were generated using the IBM SPSS Statistics program.

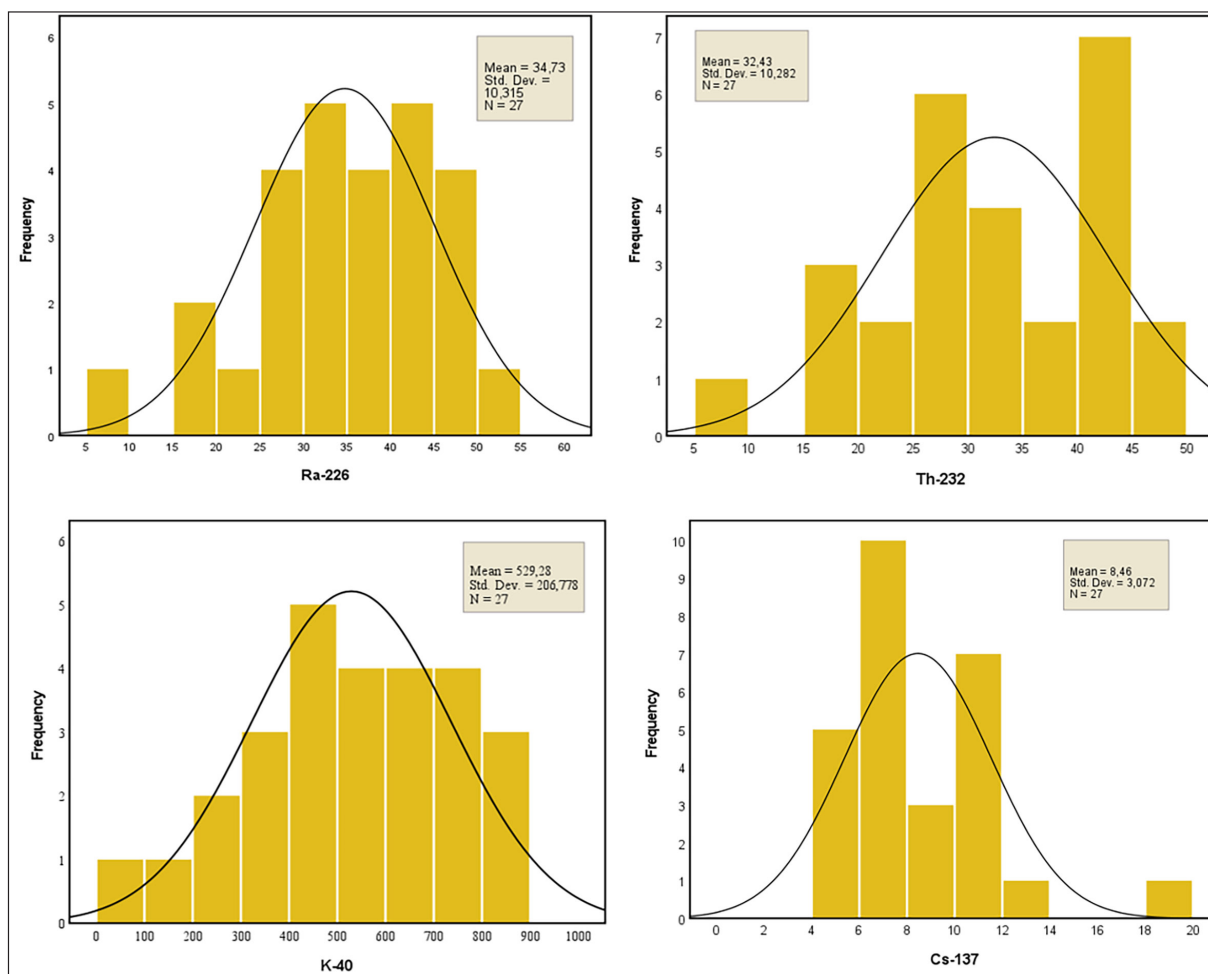


Figure 2. The frequency distributions of ^{226}Ra , ^{232}Th , ^{40}K , and ^{137}Cs radioactivity concentrations in the study area.

Table 2. Comparison the activity concentrations of ^{226}Ra , ^{232}Th , ^{40}K , and ^{137}Cs soil samples in Türkiye and several other countries

Region	^{226}Ra (Bq.kg ⁻¹)	^{232}Th (Bq.kg ⁻¹)	^{40}K (Bq.kg ⁻¹)	^{137}Cs (Bq.kg ⁻¹)	Reference
Erçel Lake, Türkiye	8.6–42.6	11.6–53.2	254.1–771.9	0.7–24.4	Yıldız et al. (2014)
Eğirdir Lake, Türkiye	34.13	27.32	363.28		Özseven et al. (2020)
East Antarctica	33	199	1150		Pal et al. (2021)
Saline Lakes, Crimea	65.68	34.95	287.42		Shadrin et al. (2020)
Qarun Lake, Egypt	10.21	11.05	927.44		Drawish et al. (2013)
Rize Türkiye	85.75	51.08	771.57	236.38	Dizman et al. (2016)
Aegean coast, Greece	9–31	9–67	426–740	0.8–2.6	Shahrokhi et al. (2021)
Gaeta Gulf, Italy	-	91.7	603.7	8.82	Desideri et al. (2002)
Brazil	62	82	179		Riberio et al. (2017)
Thailand	22.6	26.4	523.0	-	Malain et al. (2012)
East Siberian Sea, Russia	26.6	39.2	726	2.0	Ulyantsev et al. (2023)
Oguta Lake, Nigeria	47.89	55.37	1023	-	Isinkaye et al. (2015)
Iran	24.3	25.8	457.7		Kardan et al. (2017)
This study	34.73	32.43	529.28	8.46	

The dose values resulting from the natural radioactivity of the soil samples, the hazard indices (H_{in} , H_{ex}), and the ELCR were calculated as presented in Table 3.

According to Table 3, Ra_{eq} stemming from the natural radioactivity of the soil samples ranged from (28.93 to 188) Bq.kg⁻¹ with a mean of 121.86 Bq.kg⁻¹. These values fall below the WHO-recommended global mean of 370 Bq/kg (WHO 2003).

ADR for the soil samples is in the range of 13.48–89.91 nGy.h⁻¹. The mean of 57.71 nGy.h⁻¹ is below the global mean value of 60 nGy.h⁻¹ (WHO 2003). Similarly, across all samples, AEDR values with a mean of 43.13 $\mu\text{Sv.y}^{-1}$ are significantly below the global mean of 460 $\mu\text{Sv.y}^{-1}$ (UNSCEAR 2000). As seen in Table 3, H_{ex} and H_{in} both reach a maximum value of 0.33 and 0.42, respectively. Table 3 shows that the mean H_{ex} is 0.24 and the mean H_{in} is 0.34. Both of these values are

below the permitted maximum limit value of 1 (WHO 2003). The calculated maximum lifetime cancer risk value is 0.39, with a mean of 0.25. The average value does not exceed the recommended threshold of 0.29 (UNSCEAR 2000).

Table3. Dose calculations and radiological hazard parameters of the soil samples

Sample ID	Ra _{eq} (Bq.kg ⁻¹)	D (nGy.h ⁻¹)	AEDR (mSv.y ⁻¹)	H _{in}	H _{ex}	ELCR (×10 ⁻³)
1	188.63	89.91	110.26	0.65	0.51	0.39
2	156.86	74.33	91.15	0.54	0.42	0.32
3	178.34	85.01	104.25	0.62	0.48	0.36
4	149.64	71.21	87.33	0.51	0.4	0.31
5	158.67	75.35	92.41	0.55	0.43	0.32
6	164.08	78.32	96.05	0.56	0.44	0.34
7	120.58	57.18	70.12	0.42	0.33	0.25
8	85.39	40.21	49.31	0.3	0.23	0.17
9	66.11	30.8	37.78	0.23	0.18	0.13
10	59.28	27.51	33.74	0.21	0.16	0.12
11	89.2	42.29	51.86	0.32	0.24	0.18
12	63.27	29.64	36.35	0.22	0.17	0.13
13	121.13	57.28	70.25	0.42	0.33	0.25
14	103.37	48.81	59.86	0.36	0.28	0.21
15	107.59	50.85	62.36	0.37	0.29	0.22
16	124.72	58.82	72.13	0.43	0.34	0.25
17	107.35	50.9	62.43	0.38	0.29	0.22
18	151.28	71.39	87.55	0.52	0.41	0.31
19	170.3	80.31	98.49	0.59	0.46	0.34
20	147.88	69.9	85.72	0.51	0.4	0.3
21	107.01	50.67	62.14	0.37	0.29	0.22
22	116.15	55.23	67.74	0.41	0.31	0.24
23	111.72	52.8	64.76	0.39	0.3	0.23
24	95.59	45.09	55.29	0.33	0.26	0.19
25	163.44	77.59	95.15	0.57	0.44	0.33
26	153.7	73.16	89.72	0.54	0.42	0.31
27	28.93	13.48	16.54	0.1	0.08	0.06
Mean	121.86	57.71	70.77	0.42	0.33	0.25
¹ World mean	370	60	460	<1	<1	0.29

1(WHO 2003; UNSCEAR 2000)

4. Conclusion

In this research, the radioactivity levels of the natural radionuclides (²²⁶Ra, ²³²Th, and ⁴⁰K) and the artificial radionuclide (¹³⁷Cs) were investigated in soil samples collected from the coast of Arin Lake using a HPGe detector system.

The results show that the average concentration of ²²⁶Ra is lower than the global average, while ²³²Th and ⁴⁰K are higher. The high levels of ²³²Th and ⁴⁰K may be due to the volcanic nature of Süphan Volcano and the region's geological structure, especially in the use of potassium-based fertilizers. These factors contribute to the high soil concentrations observed.

Despite some elevated levels, the calculated radiological parameters, including absorbed dose rate (D), radium equivalent activity (Ra_{eq}), and annual effective dose rate (AEDR), remained within safe limits as recommended by UNSCEAR (UNSCEAR 2000). In addition, radiological hazard indices, such as the internal (H_{in}) and external (H_{ex})

hazard indices, and the excess lifetime cancer risk (ELCR) are below the permissible threshold values.

In conclusion, although certain natural radionuclides were above global averages, the overall radiological risk is minimal, indicating that the area does not pose substantial health risks according to the parameters analyzed.

Acknowledgments

This research received financial support from the Scientific Projects Department of Bitlis Eren University (BEBAP 2022.18).

References

- Abbasi, A., Zakaly, H. M., and Alotaibi, B. M. 2023. Radioactivity concentration and radiological risk assessment of beach sand along the coastline in the Mediterranean Sea. *Marine Pollution Bulletin* 195: 115527. <https://doi.org/10.1016/j.marpolbul.2023.115527>.
- Akça, S., Küçükönder, E., Karatepe, S., and Doğru, M. 2014. Radioactivity levels in some mushroom species and consequent doses. *Asian Journal of Chemistry* 26(3): 879.

- Al-Harashsheh, S., and Al-Dalabeeh, M. (2020). Measurement of radon levels in the groundwater of Al-Rusaifah City in Zarqa governorate using liquid scintillation counter. *Jordan Journal of Earth and Environmental Sciences*, 11, 98-102.
- Al-Momani, I. F., and Ali, S. M. 2024. Investigation of Heavy Metals in Indoor Dust from Irbid, Jordan. *Jordan Journal of Earth & Environmental Sciences*, 15(2).
- Al Shaaibi, M., Ali, J., Tsikouras, B., and Masri, Z. 2023. Environmental radioactivity assessment of the Brunei Darussalam coastline of the South China Sea. *Environmental Pollution* 323: 121288. <https://doi.org/10.1016/j.envpol.2023.121288>.
- Baykara, O., Karatepe, Ş., and Dođru, M. 2011. Assessments of natural radioactivity and radiological hazards in construction materials used in Elazig, Turkey. *Radiation Measurements* 46(1): 153–158. <https://doi.org/10.1016/j.radmeas.2010.11.019>.
- Canbazoglu, C., Ilter, S., Sahin Bal, S., Karatepe, S., and Dogru, M. 2018. A preliminary study on radioactivity concentrations and dose assessment of some anticarcinogenic medicinal plants used in Turkey. *Fresenius Environmental Bulletin* 27: 793–798.
- Çelik, Ş. K., and Bal, S. Ş. 2024. An evaluation of radon concentrations in Arin Lake, Bitlis. *Water, Air, & Soil Pollution* 235(2): 94.
- Desideri, D., Meli, M. A., Roselli, C., and Testa, C. 2002. Geochemical partitioning of actinides, ¹³⁷Cs and ⁴⁰K in a Tyrrhenian sea sediment sample: Comparison to stable elements. *Journal of Radioanalytical and Nuclear Chemistry* 251: 37–41.
- Dizman, S., Görtür, F. K., and Keser, R. 2016. Determination of radioactivity levels of soil samples and the excess of lifetime cancer risk in Rize Province, Turkey. *International Journal of Radiation Research* 14(3): 237–244. <https://doi.org/10.18869/acadpub.ijrr.14.3.237>.
- Gilmore, G. R. 2008. *Practical Gamma-ray Spectroscopy*, 2nd ed. John Wiley & Sons Ltd.
- Ibraheem, A. A., El-Taher, A., and Alruwaili, M. H. 2018. Assessment of natural radioactivity levels and radiation hazard indices for soil samples from Abha, Saudi Arabia. *Results in Physics* 11: 325–330.
- IAEA-TECDOC-1360. 2003. Collection and preparation of bottom sediment samples for analysis of radionuclides and trace elements. IAEA-TECDOC-1360, Vienna.
- International Commission on Radiological Protection (ICRP). 1990. Recommendations of the International Commission on Radiological Protection. In ICRP Publication 60. Pergamon Press, Annals of ICRP, Oxford.
- Isinkaye, M. O., and Emelue, H. U. 2015. Natural radioactivity measurements and evaluation of radiological hazards in sediment of Oguta Lake, South East Nigeria. *Journal of Radiation Research and Applied Sciences* 8(3): 459–469.
- Karakaya, M.Ç., Dođru, M., Karakaya, N., Vural, H.C., Kuluöztürk, F., and Bal, S.Ş. 2015. Radioactivity concentrations and dose assessments of therapeutic peloids from some Turkish spas. *Clay Minerals* 50(2): 221–232.
- Kardan, M. R., Fathabdi, N., Attarilar, A., Esmaeili-Gheshlaghi, M. T., Karimi, M., Najafi, A., and Hosseini, S. S. 2017. A national survey of natural radionuclides in soils and terrestrial radiation exposure in Iran. *Journal of Environmental Radioactivity* 178: 168–176.
- Kayakökü, H., and Dođru, M. 2017. Radioactivity analysis of soil samples taken from the western and northern shores of Lake Van, Turkey. *Applied Radiation and Isotopes* 128: 231–236.
- Kobyay, Y., Taşkın, H., Yeşilkanat, C. M., Varinliođlu, A., and Korcak, S. 2015. Natural and artificial radioactivity assessment of dam lakes sediments in Çoruh River, Turkey. *Journal of Radioanalytical and Nuclear Chemistry* 303: 287–295.
- Krieger, R. 1985. Radioactivity of construction materials. *Betonwerk Fertigteil-Technik* 47: 468–473.
- Kuluöztürk, M. F., Çelik, Ş. K., and Dođru, M. 2020. Assessment of gamma radiation levels of beach sands in Bitlis region of Lake Van. *Arabian Journal of Geosciences* 13: 1–7. <https://doi.org/10.1007/s12517-020-05600-7>.
- Malain, D., Regan, P. H., Bradley, D. A., Matthews, M., Al-Sulaiti, H. A., and Santawamaitre, T. 2012. An evaluation of the natural radioactivity in Andaman beach sand samples of Thailand after the 2004 tsunami. *Applied Radiation and Isotopes* 70(8): 1467–1474.
- Mantero, J., Thomas, R., Holm, E., Rääf, C., Vioque, I., Ruiz-Cánovas, C., and Isaksson, M. 2020. Pit lakes from Southern Sweden: Natural radioactivity and elementary characterization. *Scientific Reports* 10(1): 13712.
- Mehra, R., Kaur, S., Chand, S., Charan, C., and Mehta, M. 2021. Dosimetric assessment of primordial radionuclides in soil and groundwater of Sikar district, Rajasthan. *Journal of Radioanalytical and Nuclear Chemistry* 330: 1605–1620.
- Nergiz, H., and Durmus, A. 2017. Effects of habitat change on breeding waterbirds in Arin (Sodali) Lake, Turkey. *Applied Ecology and Environmental Research* 15(3): 1111–1118.
- ORTEC. 2006. Maestro-32: Multi-channel analyzer software, a65-b32 model. <https://www.ortec-online.com/-/media/ametekortec/manuals/a65-mnl.pdf>.
- Özden, S., and Aközcan, S. 2021. Natural radioactivity measurements and evaluation of radiological hazards in sediment of Aliğa Bay, İzmir (Turkey). *Arabian Journal of Geosciences* 14: 1–14.
- Özmen, S. F., Cesur, A., Boztosun, I., and Yavuz, M. E. L. E. K. 2014. Distribution of natural and anthropogenic radionuclides in beach sand samples from Mediterranean coast of Turkey. *Radiation Physics and Chemistry* 103: 37–44.
- Özseven, A., Akkurt, I., and Günođlu, K. 2020. Determination of some dosimetric parameters in Eğirdir Lake, Isparta, Turkey. *International Journal of Environmental Science and Technology* 17: 1503–1510.
- Pal, R., Patra, A. C., Bakshi, A. K., Dhabeekar, B., Reddy, P. J., Sengupta, P., and Sapra, B. K. 2021. Investigations on baseline levels for natural radioactivity in soils, rocks, and lakes of Larsemann Hills in East Antarctica. *Environmental Monitoring and Assessment* 193: 1–21.
- Ribeiro, F. C., da Lauria, D. C., do Rio, M. A., da Cunha, F. G., de Oliveira Sousa, W., de Albuquerque Medeiros Lima, E., and Franzen, M. 2017. Mapping soil radioactivity in the Fernando de Noronha archipelago, Brazil. *Journal of Radioanalytical and Nuclear Chemistry* 311: 577–587.
- Satyannarayana, G. V. V., Sivakumar, N. S., VidyaSagar, D., Murali, N., Rao, A. D. P., and Narayana, P. L. 2023. Measurement of natural radioactivity and radiation hazard assessment in the soil samples of Visakhapatnam, Andhra Pradesh, India. *Journal of the Indian Chemical Society* 100(1): 100856.
- Shadrin, N., Mirzoeva, N., Sidorov, I., Korotkov, A., and Anufrieva, E. 2020. Natural radionuclides in bottom sediments of the saline lakes: What factors determine their concentration? *Environmental Earth Sciences* 79(8): 168.
- Shahrokh, A., Adelikhah, M., Chalupnik, S., and Kovács, T. 2021. Multivariate statistical approach on distribution of natural and anthropogenic radionuclides and associated radiation indices along the north-western coastline of Aegean Sea, Greece. *Marine Pollution Bulletin* 163: 112009.
- Singh, K. K., and Vasudevan, S. 2021. Reconstruction of sedimentation rates based on the chronological framework of Lake Pykara, Tamil Nadu, India. *Environmental Monitoring and Assessment* 193(7): 428.
- Tucaković, I., Karanović, G., Coha, I., Pavičić-Hamer, D., and Grahek, Ž. 2023. Radionuclides in commercial children's food Ulyantsev, A., Ivannikov, S., Bratskaya, S., and Charkin, A.

2023. Radioactivity of anthropogenic and natural radionuclides in marine sediments of the Chaun Bay, east Siberian Sea. *Marine Pollution Bulletin* 195: 115582.

UNSCEAR. 2000. United Nations Scientific Committee on the Effects of Atomic Radiation: Sources and effects of ionizing radiation. Volume I: Sources; Volume II: Effects. Report to the General Assembly, with scientific annexes. United Nations Sales Publications E.00.IX.3 and E.00.IX.4, United Nations, New York.

Van, T. T., Bat, L. T., Nhan, D. D., Quang, N. H., Cam, B. D., and Hung, L. V. 2019. Estimation of radionuclide concentrations and average annual committed effective dose due to ingestion for the population in the Red River Delta, Vietnam. *Environmental Management* 63: 444–454.

WHO. 2003. World Health Organization, guidelines for drinking water quality, vol. 3-Chapter 9 draft. Switzerland, Geneva.

Yadav, M., Jindal, M. K., Bossew, P., and Ramola, R. C. 2023. Geological control of terrestrial background radiation in Garhwal Himalaya, India. *Environmental Geochemistry and Health* 45(11): 8379–8401.

Yadav, M., Jindal, M. K., and Ramola, R. C. 2023. Study of radionuclides in rock samples from Ukhimath area and its correlation with soil and water data. *Chemistry Africa* 6(4): 2165–2173.

Yıldız, N., Oto, B., Turhan, Ş., Uğur, F. A., and Gören, E. 2014. Radionuclide determination and radioactivity evaluation of surface soil samples collected along the Erçek Lake basin in eastern Anatolia, Turkey. *Journal of Geochemical Exploration* 146: 34–39.